

**ABSTRACT**

The purpose of this study was to characterize the effects of heavy-ion irradiation on the single-event latchup (SEL) performance of the INA901-SP, 65V, low-high-side, high-speed, voltage output current sense amplifier. Heavy ions with an  $LET_{EFF}$  of 76 to 93MeV-cm<sup>2</sup>/mg were used to irradiate one device with a fluence of  $1 \times 10^7$  ions / cm<sup>2</sup>. The results demonstrate that the INA901-SP is SEL-free up to  $LET_{EFF} = 93\text{MeV-cm}^2 / \text{mg}$  at 125°C.

**Table of Contents**

<b>1 Introduction</b> .....	3
<b>2 Single-Event Effects (SEE)</b> .....	4
<b>3 Device and Test Board Information</b> .....	5
<b>4 Irradiation Facility and Setup</b> .....	7
<b>5 Test Setup and Procedures</b> .....	8
<b>6 Destructive Single-Event Effects (DSEE)</b> .....	9
6.1 Single-Event Latch-up (SEL) Results.....	9
<b>7 Single-Event Transients (SET)</b> .....	10
<b>8 Event Rate Calculations</b> .....	20
<b>9 Summary</b> .....	23
<b>A References</b> .....	24

**List of Figures**

Figure 3-1. INA901-SP Pinout.....	5
Figure 3-2. INA901-SP Evaluation Board.....	5
Figure 3-3. INA901-SP Evaluation Board Schematic.....	6
Figure 5-1. Block Diagram of SEE Test Setup with the INA901-SP.....	8
Figure 6-1. Current vs Time (I vs t) Plot for $V_{IN}$ Supply Current During SEL Run 11.....	9
Figure 7-1. Histogram of the Amplitude for the Positive $V_{OUT}$ SETs on Run 4, VCM = 12V, $LET_{EFF} = 93\text{MeV}$ .....	11
Figure 7-2. Histogram of the Amplitude for the Negative $V_{OUT}$ SETs on Run 4, VCM = 12V, $LET_{EFF} = 93\text{MeV}$ .....	12
Figure 7-3. Histogram of the Pulse Width for the Positive $V_{OUT}$ SETs on Run 4, VCM = 12V, $LET_{EFF} = 93\text{MeV}$ .....	12
Figure 7-4. Histogram of the Amplitude for the Positive $V_{OUT}$ SETs on Run 6, VCM = 15V, $LET_{EFF} = 93\text{MeV}$ .....	13
Figure 7-5. Histogram of the Amplitude for the Negative $V_{OUT}$ SETs on Run # 6, VCM = 15V, $LET_{EFF} = 93\text{MeV}$ .....	13
Figure 7-6. Histogram of the Pulse Width for the Positive $V_{OUT}$ SETs on Run 6, VCM = 15V, $LET_{EFF} = 93\text{MeV}$ .....	14
Figure 7-7. Histogram of the Amplitude for the Positive $V_{OUT}$ SETs on Run 7, VCM = 48V, $LET_{EFF} = 93\text{MeV}$ .....	14
Figure 7-8. Histogram of the Amplitude for the Negative $V_{OUT}$ SETs on Run 7, VCM = 48V, $LET_{EFF} = 93\text{MeV}$ .....	15
Figure 7-9. Histogram of the Pulse Width for the Positive $V_{OUT}$ SETs on Run 7, VCM = 48V, $LET_{EFF} = 93\text{MeV}$ .....	15
Figure 7-10. Histogram of the Amplitude for the Positive $V_{OUT}$ SETs on Run 19, VCM = 12V, $LET_{EFF} = 3.44\text{MeV}$ .....	16
Figure 7-11. Histogram of the Pulse Width for the Positive $V_{OUT}$ SETs on Run 19, VCM = 12V, $LET_{EFF} = 3.44\text{MeV}$ .....	16
Figure 7-12. Histogram of the Amplitude for the Negative $V_{OUT}$ SETs on Run 20, VCM = 15V, $LET_{EFF} = 3.44\text{MeV}$ .....	17
Figure 7-13. Histogram of the Pulse Width for the Positive $V_{OUT}$ SETs on Run 20, VCM = 15V, $LET_{EFF} = 3.44\text{MeV}$ .....	17
Figure 7-14. Histogram of the Amplitude for the Positive $V_{OUT}$ SETs on Run 21, VCM = 48V, $LET_{EFF} = 3.44\text{MeV}$ .....	18
Figure 7-15. Histogram of the Pulse Width for the Positive $V_{OUT}$ SETs on Run 21, VCM = 48V, $LET_{EFF} = 3.44\text{MeV}$ .....	18
Figure 7-16. Most severe observed $V_{OUT}$ Transient, VCM = 15V, $LET_{EFF} = 93\text{MeV}$ , Run 6.....	19
Figure 8-1. Weibull Fit Curve: VCM 12V.....	20
Figure 8-2. Weibull Fit Curve - VCM 15V.....	21
Figure 8-3. Weibull Fit Curve: VCM 48V.....	22

**List of Tables**

Table 1-1. Overview Information.....	3
Table 4-1. Ion Used for SEE Characterization and Effective $LET_{EFF}$ .....	7
Table 5-1. Equipment Set and Parameters Used for SEE Testing the INA901-SP.....	8

Table 6-1. INA901-SP SEL Conditions Using <sup>165</sup> Ho With Angle-of-Incidence = 0° and 35° .....	9
Table 7-1. Summary of INA901 SET Test Condition and Results.....	10
Table 7-2. Upper Bound Cross Section for Given LET <sub>EFF</sub> for V <sub>CM</sub> 12V.....	11
Table 7-3. Upper Bound Cross Section for Given LET <sub>EFF</sub> for V <sub>CM</sub> 15V.....	11
Table 7-4. Upper Bound Cross Section for Given LET <sub>EFF</sub> for V <sub>CM</sub> 48V.....	11
Table 8-1. SEL Event Rate Calculations for Worst-Week LEO and GEO Orbits: .....	20
Table 8-2. SET Event Rate Calculations for Worst-Week LEO and GEO Orbits: VCM 12V.....	20
Table 8-3. SET Event Rate Calculations for Worst-Week LEO and GEO Orbits - VCM 15V.....	21
Table 8-4. SET Event Rate Calculations for Worst-Week LEO and GEO Orbits: VCM 48V.....	22

## Trademarks

National Instruments™ and LabVIEW™ are trademarks of National Instruments.

HP-Z4® is a registered trademark of HP Hewlett Packard Group LLC.

All trademarks are the property of their respective owners.

## 1 Introduction

The INA901-SP device is a radiation-hardened, voltage-output, current-sense amplifier that can sense drops across shunt resistors at common-mode voltages from –15V to 65V, independent of supply voltage. The INA901-SP pinouts readily enable filtering.

[Table 1-1](#) lists general device information and test conditions. For more detailed technical specifications and links to related documentation, see the [INA901-SP Radiation Hardened, –15-V to 65-V Common Mode, Unidirectional Current-Shunt Monitor data sheet](#)

**Table 1-1. Overview Information**

Description <sup>(1)</sup>	Device Information
TI Part Number	INA901-SP
SMD Number	5962-1821001VXC
Device Function	Current Sense Amplifier
Technology	LBC-SOI
Exposure Facility	Radiation Effects Facility, Cyclotron Institute, Texas A&M University
Heavy Ion Fluence per Run	$1 \times 10^7$ ions / cm <sup>2</sup>
Irradiation Temperature	125°C

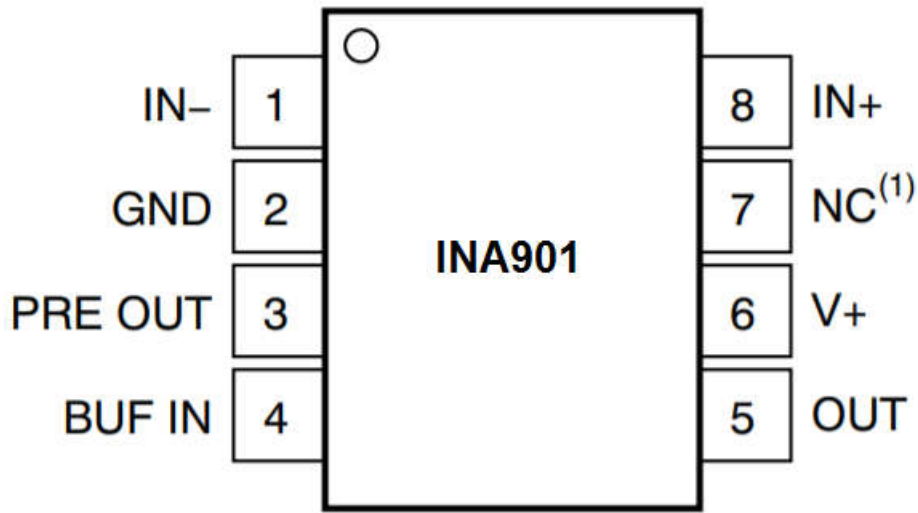
- (1) TI may provide technical, applications or design advice, quality characterization, and reliability data or service, providing these items shall not expand or otherwise affect TI's warranties as set forth in the Texas Instruments Incorporated Standard Terms and Conditions of Sale for Semiconductor Products and no obligation or liability shall arise from Semiconductor Products and no obligation or liability shall arise from TI's provision of such items.

## 2 Single-Event Effects (SEE)

The primary SEE events of interest in the INA901-SP for this report are single-event latch-up (SEL). From a risk and impact point-of-view, the occurrence of an SEL is potentially the most destructive SEE event and the biggest concern for space applications. In mixed technologies such as the LBC-SOI process used for the INA901-SP, the CMOS circuitry introduces a potential for SEL susceptibility. SEL can occur if excess current injection caused by the passage of an energetic ion is high enough to trigger the formation of a parasitic cross-coupled PNP and NPN bipolar structure (formed between the p-sub and n-well and n+ and p+ contacts). The parasitic bipolar structure initiated by a single-event creates a high-conductance path (inducing a steady-state current that is typically orders-of-magnitude higher than the normal operating current) between power and ground that persists (is *latched*) until power is removed or until the device is destroyed by the high-current state. The INA901-SP exhibited no SEL with heavy ions up to an  $LET_{EFF}$  of  $93.98\text{MeV}\cdot\text{cm}^2 / \text{mg}$  at a fluence of  $10^7$  ions /  $\text{cm}^2$  and a chip temperature of  $125^\circ\text{C}$ .

### 3 Device and Test Board Information

The INA901-SP is packaged in a 8-pin HKX package. Figure 3-1 shows the pinout diagram. The evaluation board used for the SEE characterization is shown in Figure 3-2 and schematics are shown in Figure 3-3. During the testing, the LM193AJRLQMLV device was not populated on the EVM.



Note that the package was delidded to reveal the die face for all heavy-ion testing.

Figure 3-1. INA901-SP Pinout

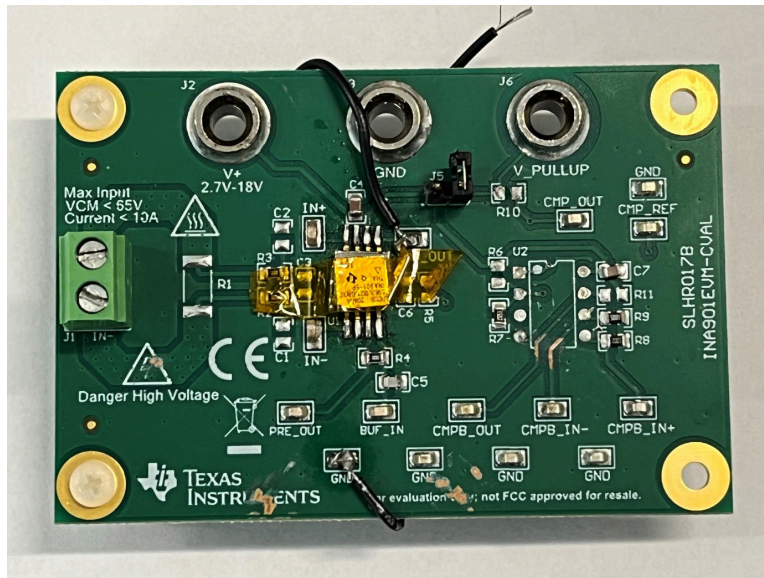
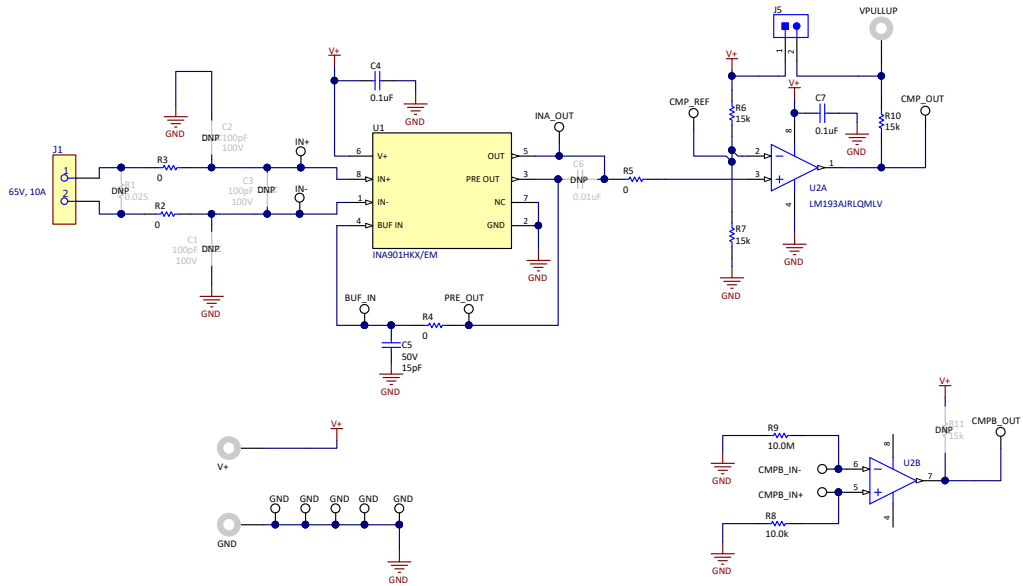


Figure 3-2. INA901-SP Evaluation Board



**Figure 3-3. INA901-SP Evaluation Board Schematic**

## 4 Irradiation Facility and Setup

The heavy-ion species used for the SEE studies on this product were provided and delivered by the Texas A&M University (TAMU) Cyclotron Radiation Effects Facility using a superconducting cyclotron and an advanced electron cyclotron resonance (ECR) ion source. At the fluxes used, ion beams had good flux stability and high irradiation uniformity over a 1in diameter circular cross-sectional area for the in-air station. Uniformity is achieved by magnetic defocusing. The flux of the beam is regulated over a broad range spanning several orders of magnitude. For the bulk of these studies, ion flux of  $10^4$  and  $10^5$  ions /  $\text{cm}^2 \times \text{s}$  were used to provide heavy-ion fluences of approximately  $3 \times 10^6$  and  $10^7$  ions /  $\text{cm}^2$ .

Figure 3-2 shows the INA901-SP test board used for the experiments at the TAMU facility. Although not visible in this photo, the beam port has a 1mil Aramica window to allow in-air testing while maintaining the vacuum within the accelerator with only minor ion energy loss. All through-hole test points were soldered backwards for access of the signals while having enough room to change the angle of incidence and maintaining the 40mm distance to the die. The in-air gap between the device and the ion beam port window was maintained at 40mm for all runs.

**Table 4-1. Ion Used for SEE Characterization and Effective LET<sub>EFF</sub>**

Ion Type	Angle of Incidence	Flux (ions × cm <sup>2</sup> / mg)	Fluence (Number of ions)	LET <sub>EFF</sub> (MeV-cm <sup>2</sup> / mg)	Notes
Ho	0°	1.00E+05	1.00E+07	76	SEL, No Latch-Up
Ho	35°	1.00E+05	1.00E+07	93	SEL,35° rotation of unit. No Latch-Up
Ho	35°	1.00E+04	1.00E+06	93	SET,35° rotation of unit.
Ho	0°	1.00E+04	1.00E+06	76	SET
Ag	0°	1.00E+04	1.00E+06	48	SET
Ag	35°	1.00E+04	1.00E+06	60	SET,35° rotation of unit.
Ne	35°	1.00E+04	1.00E+06	3.44	SET,35° rotation of unit.
Ne	0°	1.00E+04	1.00E+06	2.8	SET

## 5 Test Setup and Procedures

SEE testing was performed on a INA901-SP device mounted on a INA901EVM-CVAL.

For SEL testing, the device was powered up to the maximum recommended common mode voltage of 65V and a supply voltage of 16V.

For the SET characterization, the device was powered up to 12V, characterized over three common mode voltages - 12V, 15V, and 48V. A differential voltage of 300mV was applied between the IN- and IN+ pins to set the output at 6V (half the supply voltage). The SET events were monitored using one National Instruments™ (NI) PXIe-5172 scope card. The scope was used to monitor and trigger from OUT, using a window trigger at approximately  $6V \pm 180mV$  ( $\pm 3\%$ ) from the top of the noise floor.

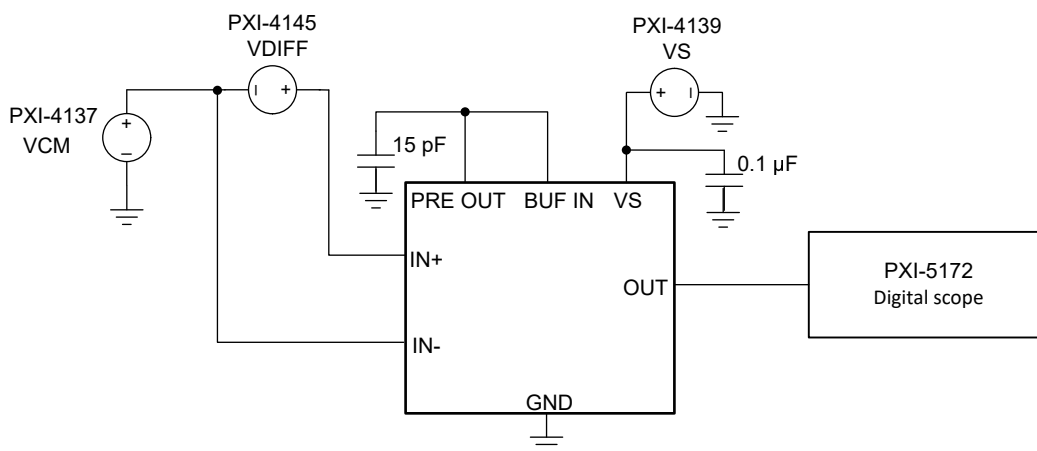
All equipment was controlled and monitored using a custom-developed LabVIEW™ program (PXI-RadTest) running on a HP-Z4® desktop computer. The computer communicates with the PXI chassis through an MXI controller and NI PXIe-8381 remote control module.

Figure 5-1 shows a block diagram of the setup used for SEE testing of the INA901-SP. Table 5-1 lists the connections, limits, and compliance values used during the testing. A die temperature of 125°C was used for SEL and was achieved with the use of a convection heat gun aimed at the die. For SET testing, the device was tested at room temperature. No cooling or heating was applied to the DUT.

**Table 5-1. Equipment Set and Parameters Used for SEE Testing the INA901-SP**

Connection Name	Equipment Used	Capability	Compliance	Range of Values Used
VCM	NI-PXIe 4137 PS	15A	10A	12V, 15V, 48V, 65V
VDIFF	NI-PXIe 4145 PS	15A	10A	300mV
OUT	NI-PXIe 5172 Digitizer Scope (Channel 0)	100MS / s	—	2MS / s
V+	NI-PXIe 4139 PS	15A	10A	12V, 16V

All boards used for SEE testing were fully checked for functionality. Dry runs were also performed to make sure that the test system was stable under all bias and load conditions prior to being taken to the TAMU facility. During the heavy-ion testing, the LabVIEW control program powered up the INA901-SP device and set the external sourcing and monitoring functions of the external equipment. After functionality and stability was confirmed, the beam shutter was opened to expose the device to the heavy-ion beam. The shutter remained open until the target fluence was achieved (determined by external detectors and counters). During irradiation, the NI scope card continuously monitored the signals. When the output voltage exceeded  $6V \pm 180mV$  ( $V_{OUT,NOM} \pm 3\%$ ) window trigger, a data capture was initiated. In addition to monitoring the voltage levels of the scope, the VS current was monitored at all times. No sudden increases in current were observed (outside of normal fluctuations) on any of the test runs and indicated that no SEL events occurred during any of the tests.



**Figure 5-1. Block Diagram of SEE Test Setup with the INA901-SP**

## 6 Destructive Single-Event Effects (DSEE)

### 6.1 Single-Event Latch-up (SEL) Results

During SEL characterization, the device was heated using forced hot air, maintaining the die temperature at 125°C. The ion used for the SEL testing was Ho(<sup>165</sup>Ho) with an angle of incidence of 0° and 35° for an LET<sub>EFF</sub> = 76 and 93MeV-cm<sup>2</sup> / mg, respectively. A flux of approximately 10<sup>5</sup> ions / cm<sup>2</sup>-s and a fluence of approximately 10<sup>7</sup> ions were used for all five runs. Run duration to achieve this fluence was approximately 120 seconds. The common mode voltage was set to the recommended maximum at 65V with a supply voltage of 16V. No SEL events were observed during all seven runs shown in Table 6-1. Figure 6-1 shows a typical plot of the current versus time.

**Table 6-1. INA901-SP SEL Conditions Using <sup>165</sup>Ho With Angle-of-Incidence = 0° and 35°**

Run Number	Distance (mm)	Temperature (°C)	Ion	Angle	FLUX (ions × cm <sup>2</sup> / mg)	Fluence (Number of ions)	LET <sub>EFF</sub> (MeV × cm <sup>2</sup> / mg)
3	40	125	Ho	0°	1.00E+05	1.00e+07	76
4	40	125	Ho	0°	1.00E+05	1.00E+07	76
6	40	125	Ho	35°	1.00E+05	1.00E+07	93
10	40	125	Ho	35°	1.00E+05	1.00E+07	93
11	40	125	Ho	35°	1.00E+05	1.00E+07	93

No SEL events were observed, indicating that the INA901-SP is SEL-immune at LET<sub>EFF</sub> = 93MeV-cm<sup>2</sup> / mg and T = 125°C.

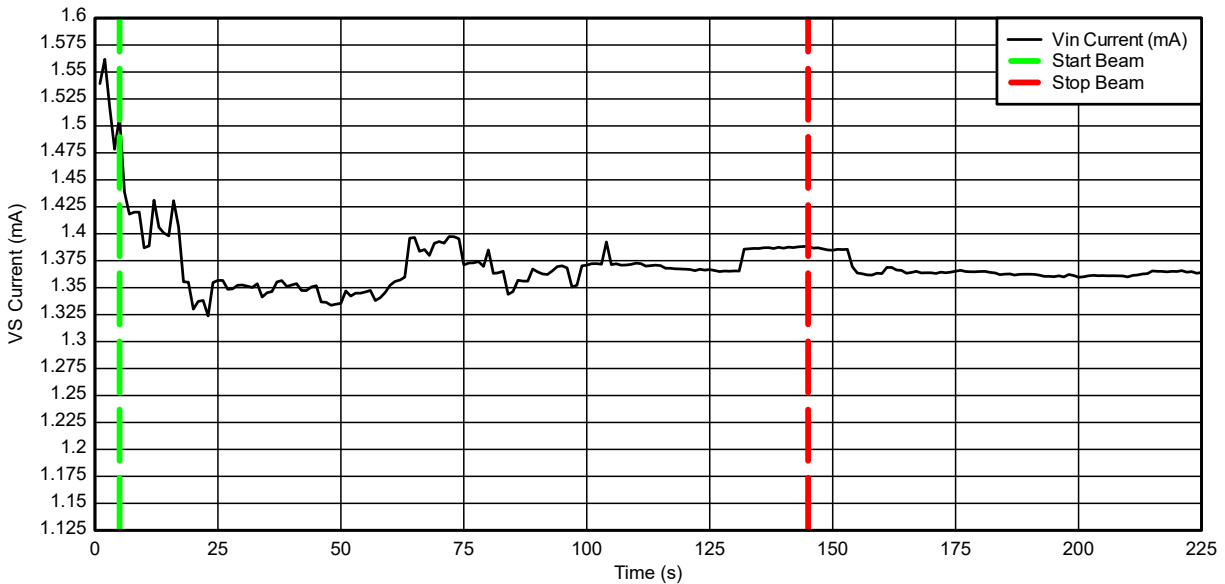


**Figure 6-1. Current vs Time (I vs t) Plot for V<sub>IN</sub> Supply Current During SEL Run 11**

## 7 Single-Event Transients (SET)

SETs are defined as heavy-ion-induced transients upsets on the OUT pin of the INA901-SP. SET testing was performed at room temperature (no external temperature control applied). The highest energy ion used for the SET testing was a Holmium ( $^{67}\text{Ho}$ ) ion with an angle-of-incidence of  $35^\circ$  for an  $\text{LET}_{\text{EFF}} = 93\text{MeV} \times \text{cm}^2 / \text{mg}$ . Flux of approximately  $10^4$  ions /  $\text{cm}^2 \times \text{s}$  and a fluence of approximately  $1 \times 10^6$  ions /  $\text{cm}^2$ .

$V_{\text{OUT}}$  SETs were characterized using a window trigger of  $6\text{V} \pm 180\text{mV}$  ( $\pm 3\%$ ) around the output voltage. The devices were characterized at three different  $V_{\text{CM}}$  levels of 12V, 15V, and 48V. The IN- pin was set to  $V_{\text{CM}}$  with a 300mV differential supply between IN- and IN+. The  $V_{\text{CC}}$  supply was set to 12V for all ion runs.

To capture the SETs a NI-PXI-5172 scope card was used to continuously monitor the OUT. The output voltage was monitored by using the INA\_OUT test point on the EVM.

The scope triggering from OUT was programmed to record 10k samples with a sample rate of 2M samples per second (S / s) in case of an event (trigger).

Under heavy-ions, the INA901-SP transient upsets that are all recoverable without any need for external intervention such as a power down or reset. There were two distinct signatures seen on the output of the INA901-SP.

Test conditions and results are listed in [Table 7-1](#).

**Table 7-1. Summary of INA901 SET Test Condition and Results**

Run Number	Unit Number	$V_{\text{S}}$ (V)	$V_{\text{CM}}$ (V)	$V_{\text{DIFF}}$ (V)	Distance (mm)	Ion	Angle ( $^\circ$ )	Flux (ions $\times$ $\text{cm}^2 / \text{mg}$ )	Fluence (Number of ions)	$\text{LET}_{\text{EFF}}$ (MeV $\times$ $\text{cm}^2 / \text{mg}$ )	Output Events
4	2	12V	12V	0.3	40	Ho	$35^\circ$	1.00E+04	1.00E+06	93	1147
6	2	12V	15V	0.3	40	Ho	$35^\circ$	1.00E+04	1.00E+06	93	1241
7	2	12V	48V	0.3	40	Ho	$35^\circ$	1.00E+04	1.00E+06	93	1250
8	2	12V	12V	0.3	40	Ho	$0^\circ$	1.00E+04	1.00E+06	75	1141
9	2	12V	15V	0.3	40	Ho	$0^\circ$	1.00E+04	1.00E+06	75	1093
10	2	12V	48V	0.3	40	Ho	$0^\circ$	1.00E+04	1.00E+06	75	1189
11	2	12V	12V	0.3	40	Ag	$0^\circ$	1.00E+04	1.00E+06	48	697
13	2	12V	15V	0.3	40	Ag	$0^\circ$	1.00E+04	1.00E+06	48.47	728
14	2	12V	48V	0.3	40	Ag	$0^\circ$	1.00E+04	1.00E+06	48	808
16	2	12V	12V	0.3	40	Ag	$35^\circ$	1.00E+04	1.00E+06	60	823
17	2	12V	15V	0.3	40	Ag	$35^\circ$	1.00E+04	1.00E+06	60	808
18	2	12V	48V	0.3	40	Ag	$35^\circ$	1.00E+04	1.00E+06	59.8	982
19	2	12V	12V	0.3	40	Ne	$35^\circ$	1.00E+04	1.00E+06	3.44	1
20	2	12V	15V	0.3	40	Ne	$35^\circ$	1.00E+04	1.00E+06	3.44	4
21	2	12V	48V	0.3	40	Ne	$35^\circ$	1.00E+04	1.00E+06	3.44	3
22	2	12V	12V	0.3	40	Ne	$0^\circ$	1.00E+04	1.00E+06	2.8	0
23	2	12V	15V	0.3	40	Ne	$0^\circ$	1.00E+04	1.00E+06	2.8	2
24	2	12V	48V	0.3	40	Ne	$0^\circ$	1.00E+04	1.00E+06	2.8	2

Using the MFTF method shown in [Single-Event Effects \(SEE\) Confidence Interval Calculations](#), the upper-bound cross-section (using a 95% confidence level) is calculated for the different SETs as listed in [Table 7-2](#), [Table 7-3](#), and [Table 7-4](#).

**Table 7-2. Upper Bound Cross Section for Given LET<sub>EFF</sub> for V<sub>CM</sub> 12V**

LET <sub>EFF</sub> (MeV cm <sup>2</sup> / mg)	Upper Bound Cross Section (cm <sup>2</sup> / device)
93	1.22E-03
76	1.21E-03
60	7.51E-04
48	8.81E-04
3.44	5.57E-06
2.8	3.69E-06

**Table 7-3. Upper Bound Cross Section for Given LET<sub>EFF</sub> for V<sub>CM</sub> 15V**

LET <sub>EFF</sub> (MeV cm <sup>2</sup> / mg)	Upper Bound Cross Section (cm <sup>2</sup> / device)
93	1.31E-03
76	1.16E-03
60	7.83E-04
48	8.66E-04
3.44	1.02E-05
2.8	7.22E-06

**Table 7-4. Upper Bound Cross Section for Given LET<sub>EFF</sub> for V<sub>CM</sub> 48V**

LET <sub>EFF</sub> (MeV cm <sup>2</sup> /mg)	Upper Bound Cross Section (cm <sup>2</sup> / device)
93	1.32E-03
76	1.26E-03
60	8.66E-04
48	1.05E-03
3.4	8.77E-06
2.8	7.22E-06

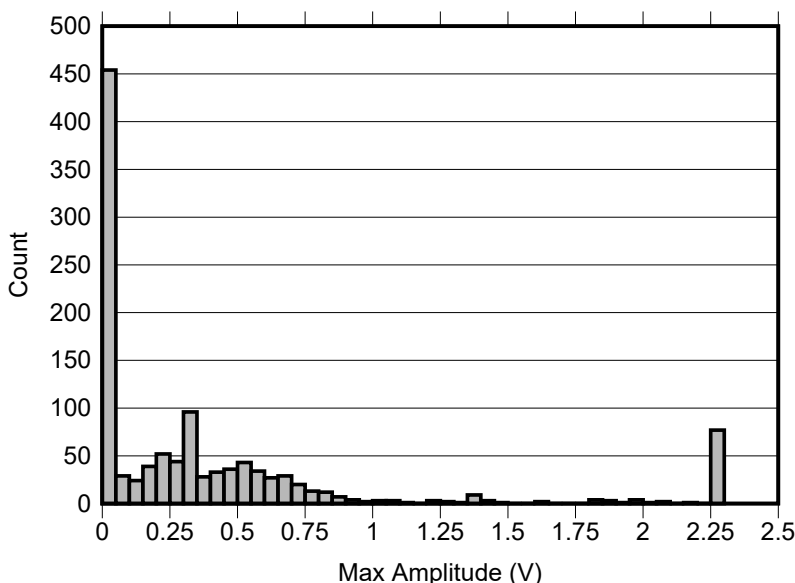


**Figure 7-1. Histogram of the Amplitude for the Positive V<sub>OUT</sub> SETs on Run 4, V<sub>CM</sub> = 12V, LET<sub>EFF</sub> = 93MeV**

Transients greater than 2.25V above the nominal output were limited by the measurement range of the digitizer. These limitations did not exist for negative transient which showed these disturbances can be as high as 5.6V.

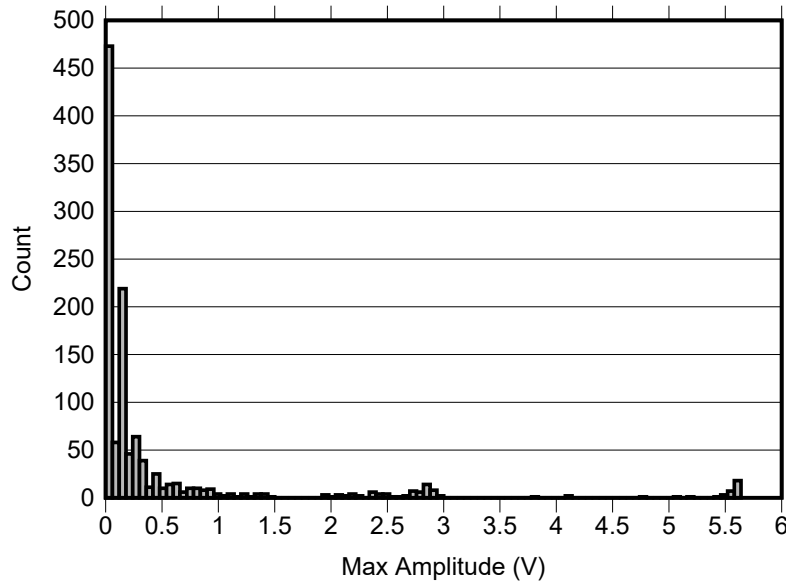


Figure 7-2. Histogram of the Amplitude for the Negative  $V_{OUT}$  SETs on Run 4,  $V_{CM} = 12V$ ,  $LET_{EFF} = 93MeV$

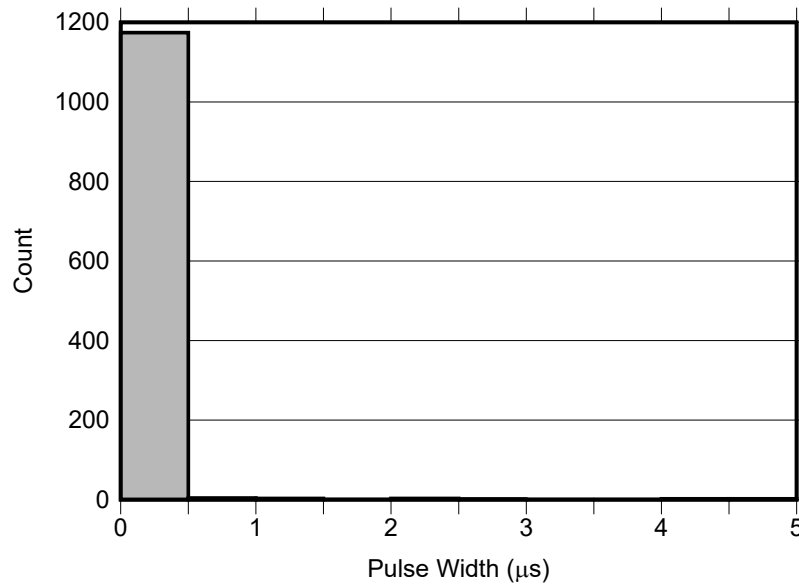
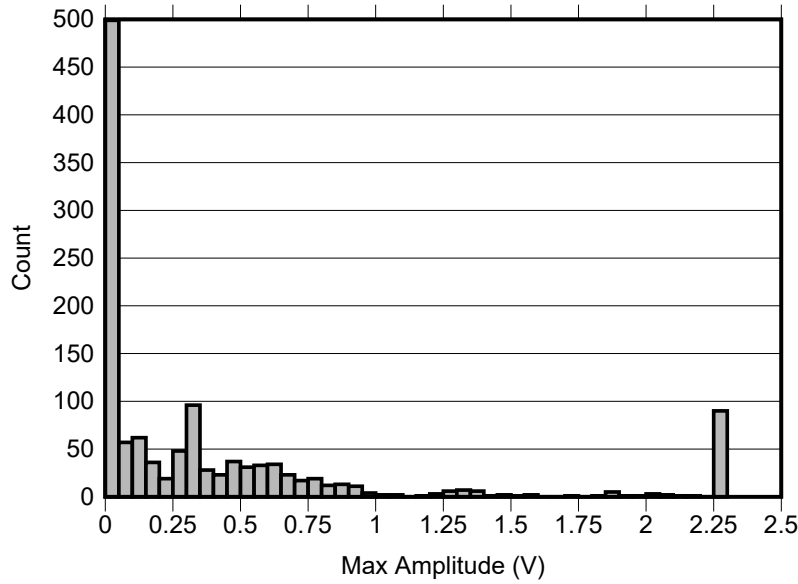
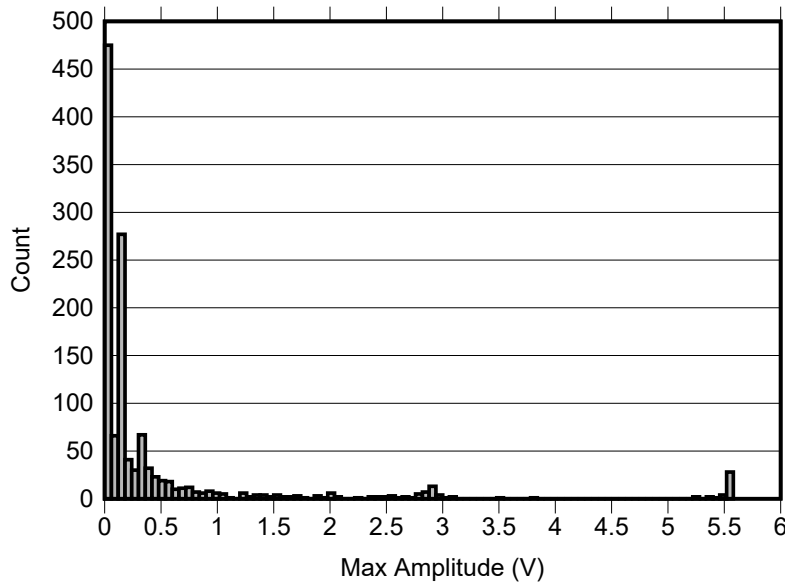


Figure 7-3. Histogram of the Pulse Width for the Positive  $V_{OUT}$  SETs on Run 4,  $V_{CM} = 12V$ ,  $LET_{EFF} = 93MeV$



**Figure 7-4. Histogram of the Amplitude for the Positive  $V_{OUT}$  SETs on Run 6,  $V_{CM} = 15V$ ,  $LET_{EFF} = 93MeV$**

Transients greater than 2.25V above the nominal output were limited by the measurement range of the digitizer. These limitations did not exist for negative transient which showed these disturbances can be as high as 5.6V.



**Figure 7-5. Histogram of the Amplitude for the Negative  $V_{OUT}$  SETs on Run # 6,  $V_{CM} = 15V$ ,  $LET_{EFF} = 93MeV$**

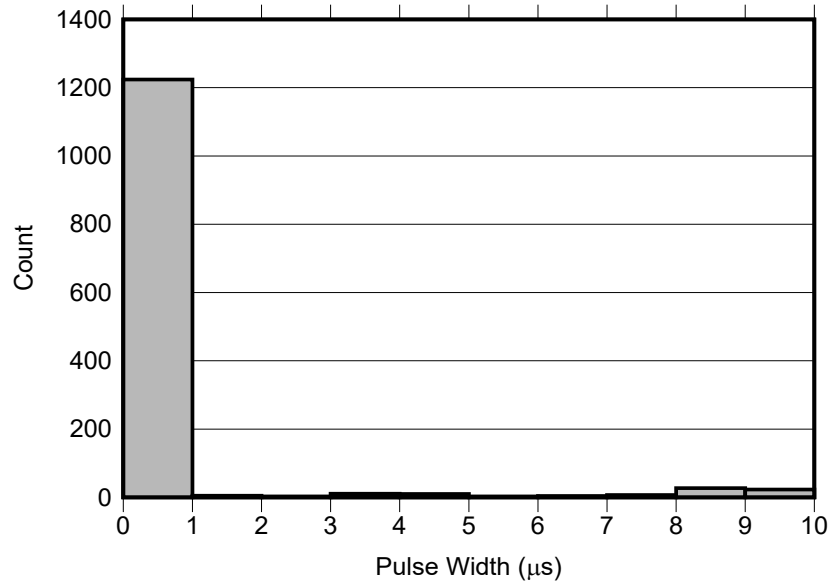


**Figure 7-6. Histogram of the Pulse Width for the Positive  $V_{OUT}$  SETs on Run 6,  $V_{CM} = 15V$ ,  $LET_{EFF} = 93MeV$**

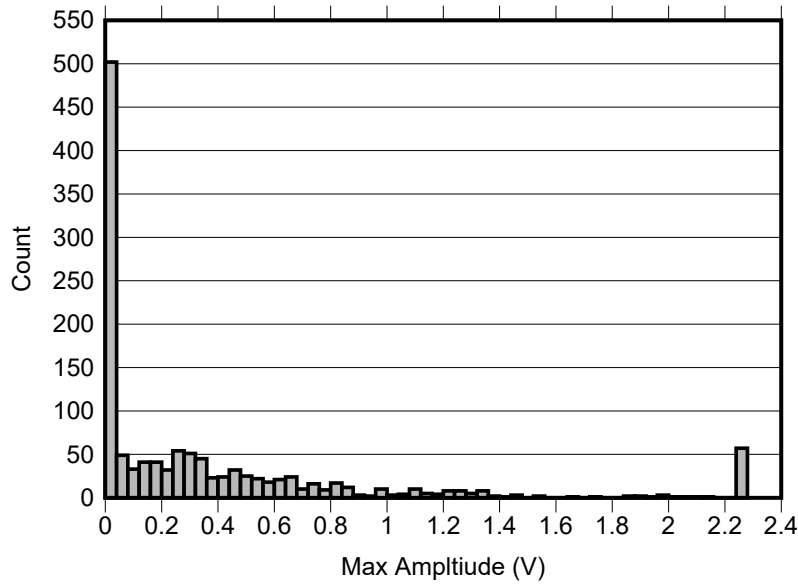


**Figure 7-7. Histogram of the Amplitude for the Positive  $V_{OUT}$  SETs on Run 7,  $V_{CM} = 48V$ ,  $LET_{EFF} = 93MeV$**

Transients greater than 2.25V above the nominal output were limited by the measurement range of the digitizer. These limitations did not exist for negative transient which showed these disturbances can be as high as 5.6V.

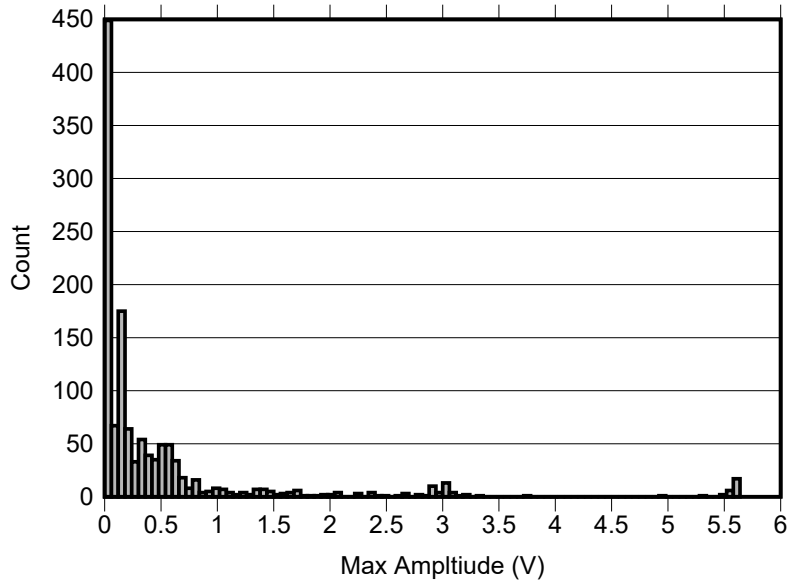


**Figure 7-8. Histogram of the Amplitude for the Negative  $V_{OUT}$  SETs on Run 7,  $V_{CM} = 48V$ ,  $LET_{EFF} = 93MeV$**

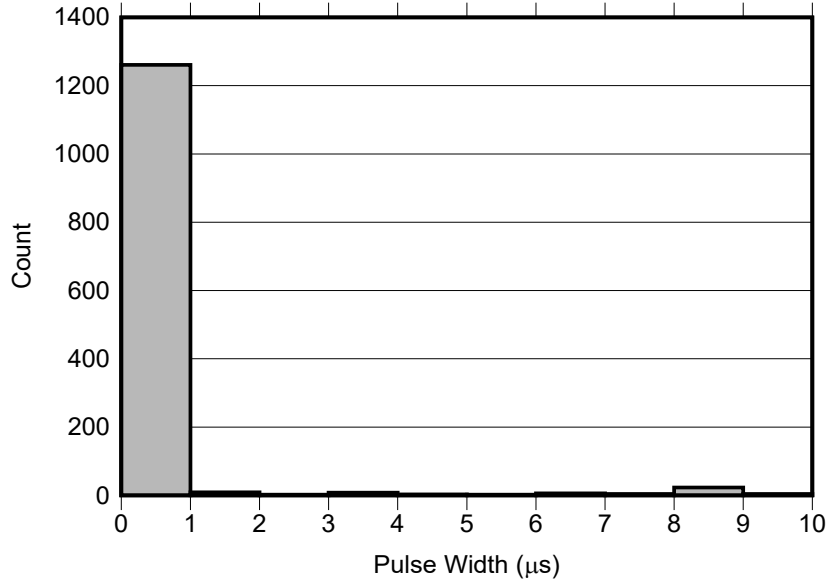


**Figure 7-9. Histogram of the Pulse Width for the Positive  $V_{OUT}$  SETs on Run 7,  $V_{CM} = 48V$ ,  $LET_{EFF} = 93MeV$**

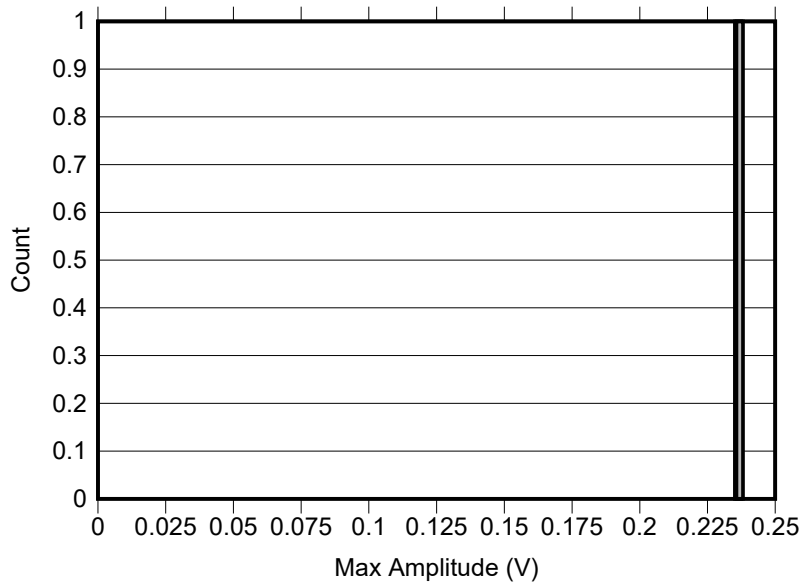


**Figure 7-10. Histogram of the Amplitude for the Positive  $V_{OUT}$  SETs on Run 19,  $V_{CM} = 12V$ ,  $LET_{EFF} = 3.44MeV$**

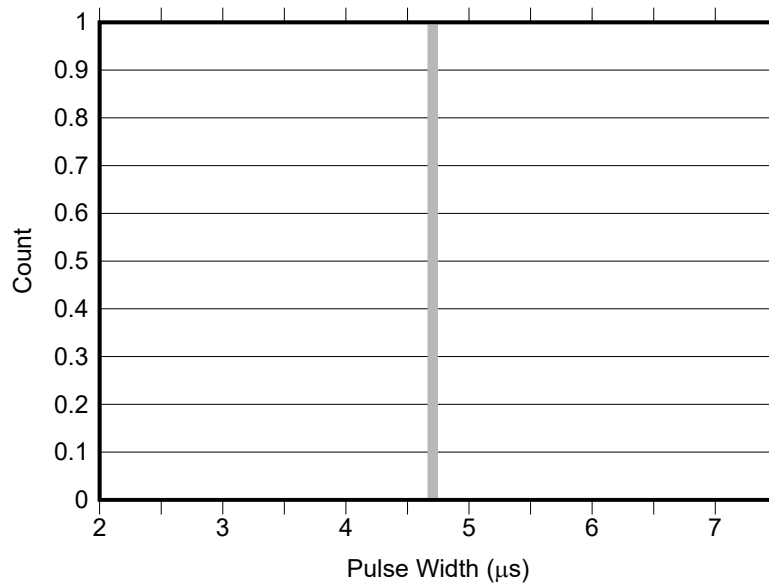


**Figure 7-11. Histogram of the Pulse Width for the Positive  $V_{OUT}$  SETs on Run 19,  $V_{CM} = 12V$ ,  $LET = 3.44MeV$**

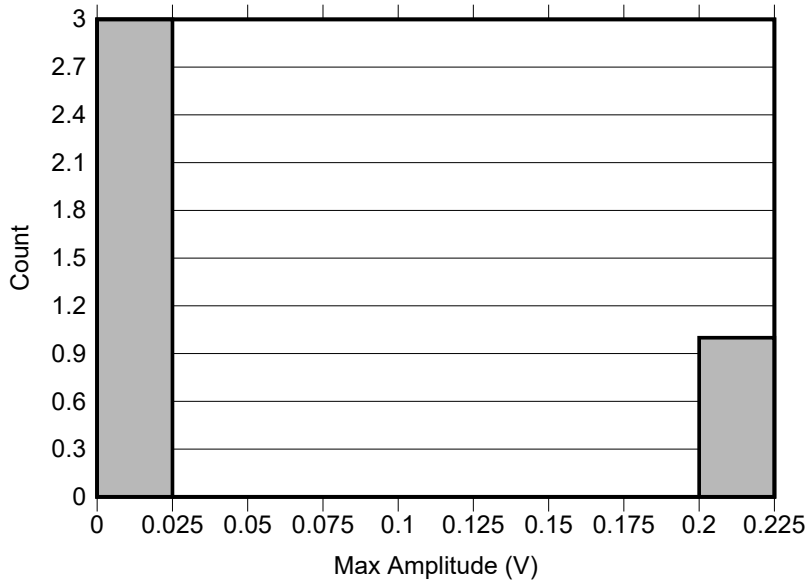


**Figure 7-12. Histogram of the Amplitude for the Negative  $V_{OUT}$  SETs on Run 20, VCM = 15V, LET= 3.44MeV**

There were no positive transients for Run 20.

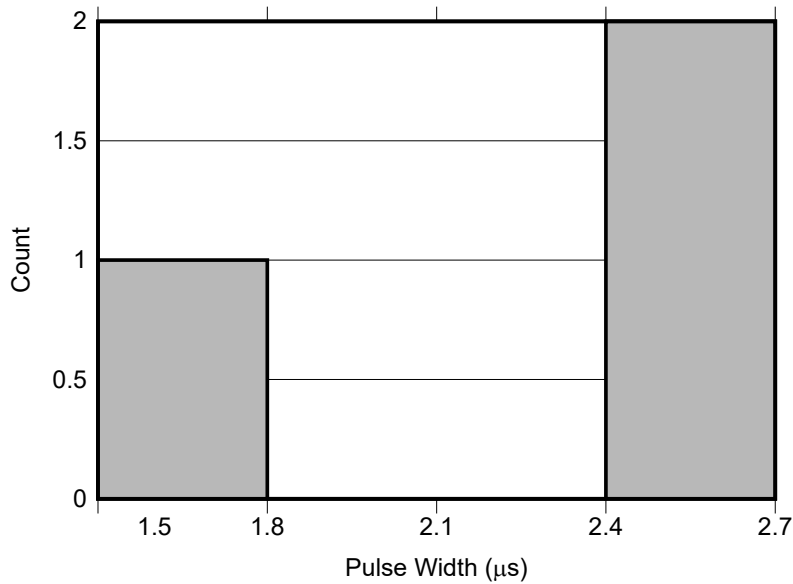


**Figure 7-13. Histogram of the Pulse Width for the Positive  $V_{OUT}$  SETs on Run 20, VCM = 15V, LET<sub>EFF</sub>= 3.44MeV**

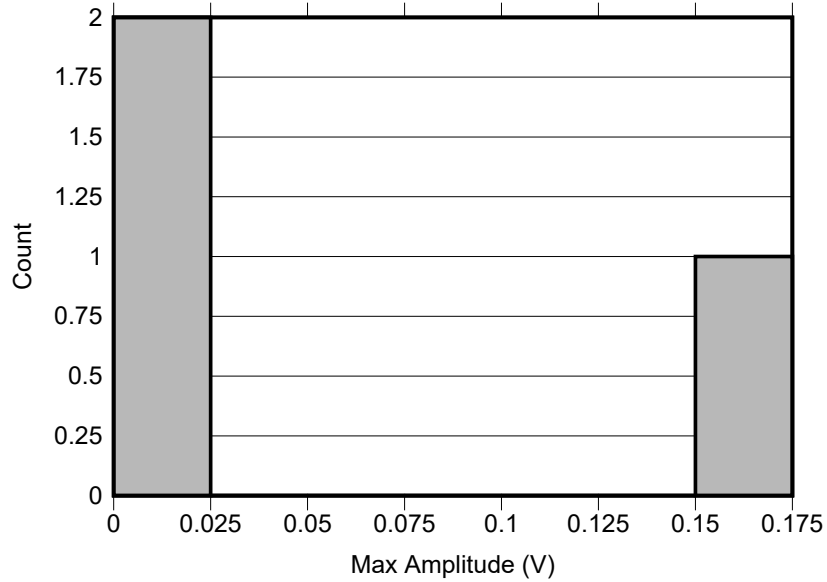


**Figure 7-14. Histogram of the Amplitude for the Positive  $V_{OUT}$  SETs on Run 21,  $V_{CM} = 48V$ ,  $LET_{EFF} = 3.44MeV$**

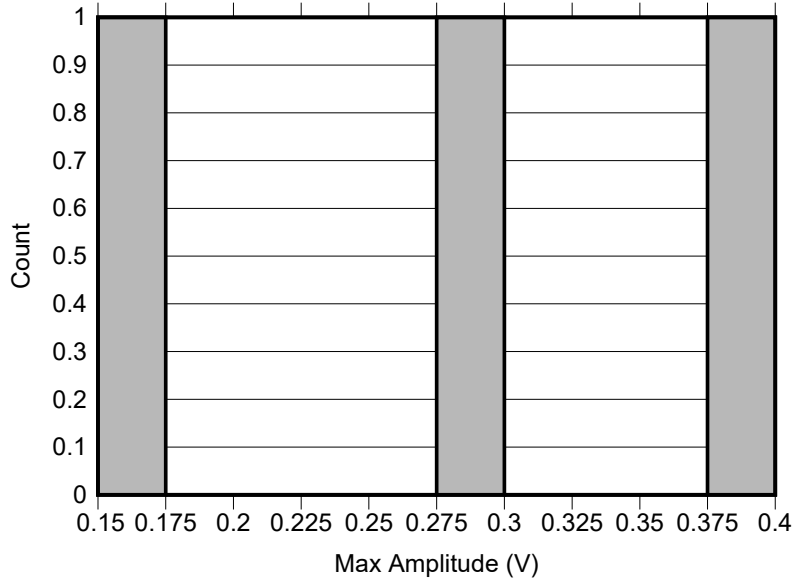


**Figure 7-15. Histogram of the Pulse Width for the Positive  $V_{OUT}$  SETs on Run 21,  $V_{CM} = 48V$ ,  $LET_{EFF} = 3.44MeV$**

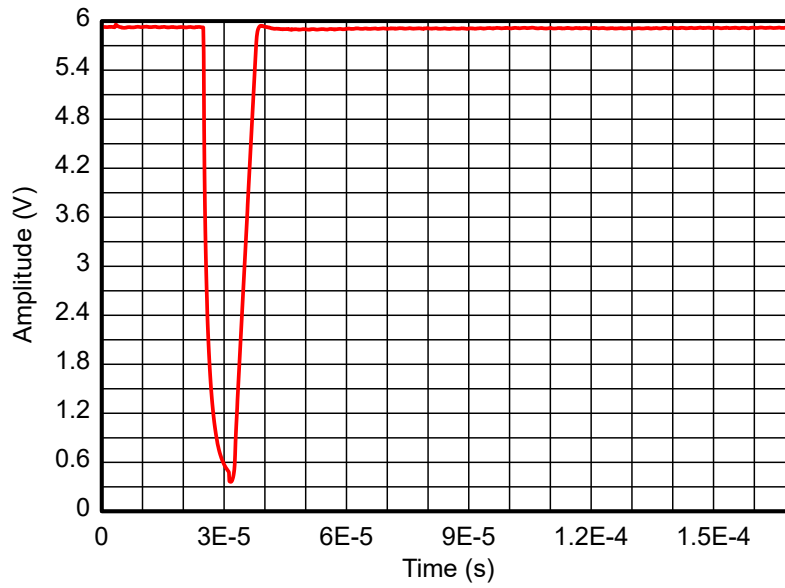


Figure 7-16. Most severe observed VOUT Transient, VCM = 15V, LET<sub>EFF</sub> = 93MeV, Run 6

## 8 Event Rate Calculations

Event rates were calculated for LEO(ISS) and GEO environments by combining CREME96 orbital integral flux estimations and simplified SEE cross-sections according to methods shown in [Heavy Ion Orbital Environment Single-Event Effects Estimations](#). Assume a minimum shielding configuration of 100mils (2.54mm) of aluminum, and *worst-week* solar activity (this is similar to a 99% upper bound for the environment). Using the 95% upper-bounds, the event rate calculation for the SEL is shown in [Table 8-1](#). **It is important to note that this number is for reference since no SEL events were observed.** SET orbit rate for the output at VIN = 12V with VCM = 12V, 15V, and 48V is shown in [Table 8-2](#), [Table 8-3](#), and [Table 8-4](#).

**Table 8-1. SEL Event Rate Calculations for Worst-Week LEO and GEO Orbits:**

Orbit Type	Onset LET <sub>EFF</sub> (MeV-cm <sup>2</sup> / mg)	CREME96 Integral FLUX ( / day / cm <sup>2</sup> )	σSAT (cm <sup>2</sup> )	Event Rate ( / day)	Event Rate (FIT)	MTBE (Years)
LEO (ISS)	2.8	5.29E-07	1.23E-07	6.5E-14	2.71E-06	4.21E+10
GEO		1.38E-06		1.7E-13	7.08E-06	1.61E+10

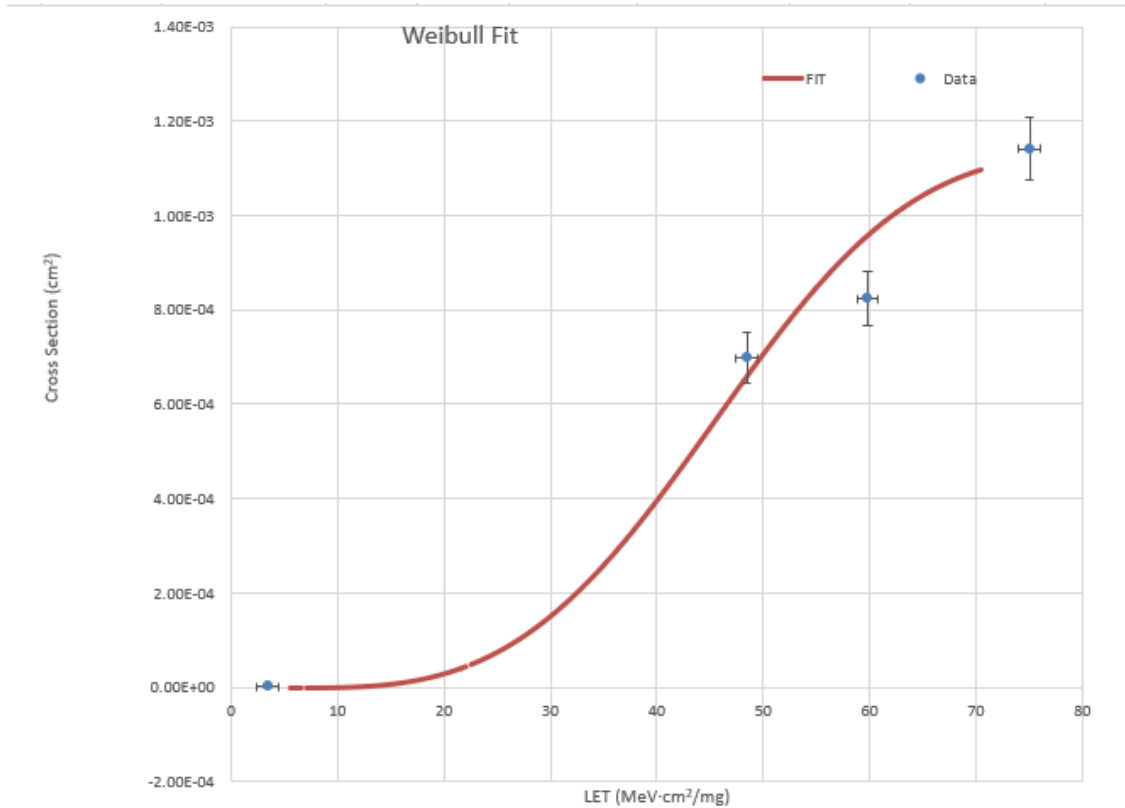


**Figure 8-1. Weibull Fit Curve: VCM 12V**

**Table 8-2. SET Event Rate Calculations for Worst-Week LEO and GEO Orbits: VCM 12V**

Orbit Type	Onset LET <sub>EFF</sub> (MeV-cm <sup>2</sup> / mg)	CREME96 Integral FLUX ( / day / cm <sup>2</sup> )	σSAT (cm <sup>2</sup> )	Event Rate ( / day)	Event Rate (FIT)	MTBE (Years)
LEO (ISS)	2.8	3.36E+02	1.22E-03	4.08E-01	1.70E+07	6.71E-03
GEO		3.22E+03		3.92E+00	1.63E+08	6.99E-04

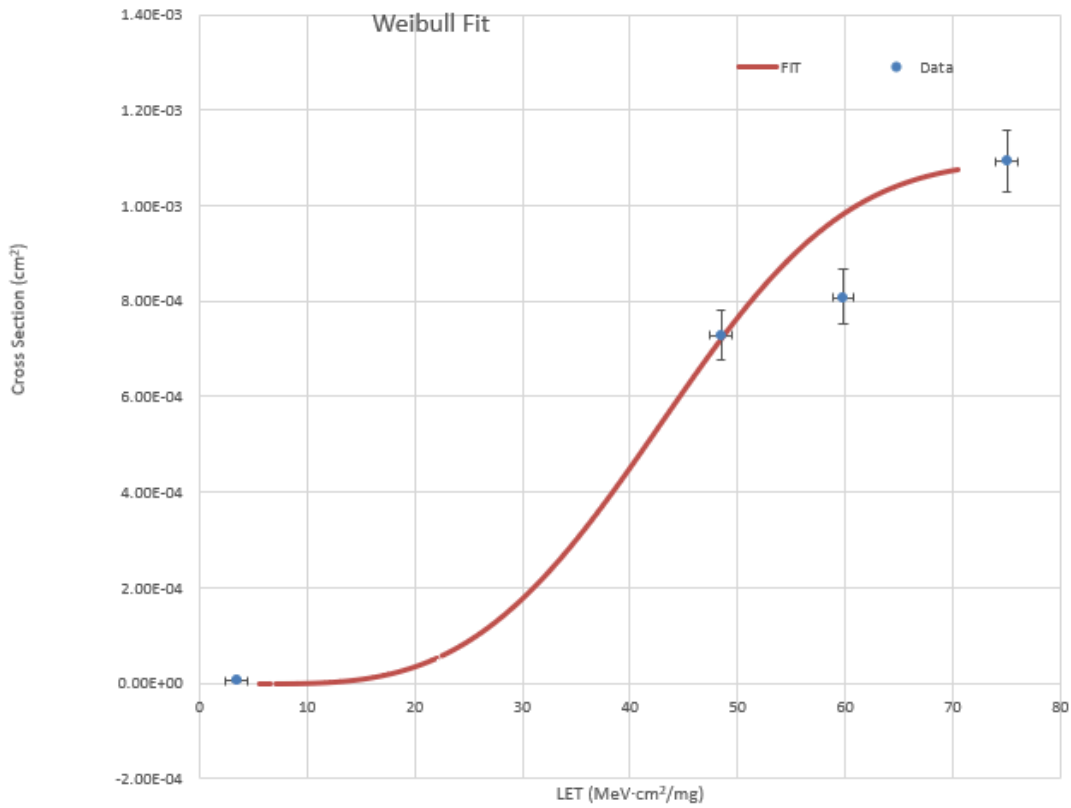


**Figure 8-2. Weibull Fit Curve - VCM 15V**

**Table 8-3. SET Event Rate Calculations for Worst-Week LEO and GEO Orbits - VCM 15V**

Orbit Type	Onset LET <sub>EFF</sub> (MeV·cm <sup>2</sup> / mg)	CREME96 Integral FLUX ( / day / cm <sup>2</sup> )	σSAT (cm <sup>2</sup> )	Event Rate ( / day)	Event Rate (FIT)	MTBE (Years)
LEO (ISS)	2.8	3.36E+02	1.31E-03	4.41E-01	1.84E+07	6.21E-03
GEO		3.22E+03		4.23E+00	1.76E+08	6.48E-04

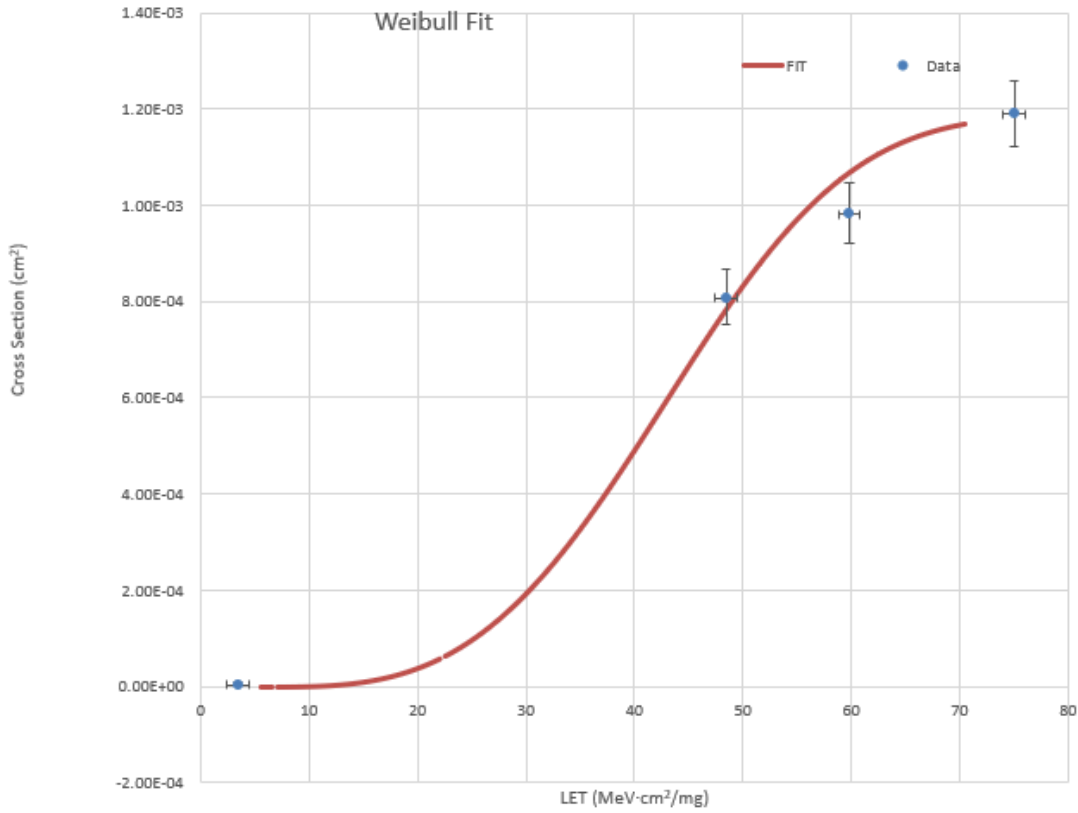


Figure 8-3. Weibull Fit Curve: VCM 48V

Table 8-4. SET Event Rate Calculations for Worst-Week LEO and GEO Orbits: VCM 48V

Orbit Type	Onset LET <sub>EFF</sub> (MeV·cm <sup>2</sup> /mg)	CREME96 Integral FLUX ( / day / cm <sup>2</sup> )	σSAT (cm <sup>2</sup> )	Event Rate ( / day)	Event Rate (FIT)	MTBE (Years)
LEO (ISS)	2.8	3.36E+02	1.32E-03	4.44E-01	1.85E+07	6.17E-03
GEO		3.22E+03		4.26E+00	1.77E+08	6.43E-04

## 9 Summary

The purpose of this study was to characterize the effect of heavy-ion irradiation on the single-event effect (SEE) performance of the INA901-SP current sense amplifier. Heavy-ions ranging from  $LET_{EFF} = 2.8$  to  $LET_{EFF} = 93\text{MeV} \times \text{cm}^2 / \text{mg}$  were used for the SEE characterization campaign. Flux of  $10^4$  and  $10^5$  ions/ $\text{cm}^2 \times \text{s}$  and fluences ranging from  $1 \times 10^6$  to  $3 \times 10^6$  ions /  $\text{cm}^2$  per run were used for the characterization. The SEE results demonstrated that the INA901-SP is SEL-free up to  $LET_{EFF} = 93\text{MeV} \times \text{cm}^2 / \text{mg}$  and across the full electrical specifications. Transients for  $LET_{EFF}$  levels from 2.8 to  $93\text{MeV} \times \text{cm}^2 / \text{mg}$  on OUT are shown and discussed. CREME96-based worst-week event-rate calculations for LEO(ISS) and GEO orbits for the DSEE are shown for reference.

## A References

1. M. Shoga and D. Binder, "Theory of Single Event Latchup in Complementary Metal-Oxide Semiconductor Integrated Circuits", *IEEE Trans. Nucl. Sci.*, Vol. 33(6), Dec. 1986, pp. 1714-1717.
2. G. Bruguier and J. M. Palau, "Single particle-induced latchup", *IEEE Trans. Nucl. Sci.*, Vol. 43(2), Mar. 1996, pp. 522-532.
3. G. H. Johnson, J. H. Hohl, R. D. Schrimpf and K. F. Galloway, "Simulating single-event burnout of n-channel power MOSFET's," in IEEE Transactions on Electron Devices, vol. 40, no. 5, pp. 1001-1008, May 1993.
4. J. R. Brews, M. Allenspach, R. D. Schrimpf, K. F. Galloway, J. L. Titus and C. F. Wheatley, "A conceptual model of a single-event gate-rupture in power MOSFETs," in IEEE Transactions on Nuclear Science, vol. 40, no. 6, pp. 1959-1966, Dec. 1993.
5. G. H. Johnson, R. D. Schrimpf, K. F. Galloway, and R. Koga, "Temperature dependence of single event burnout in n-channel power MOSFETs [for space application]," *IEEE Trans. Nucl. Sci.*, 39(6), Dec. 1992, pp. 1605-1612.
6. Texas A&M University, Cyclotron Institute, [Texas A&M University Cyclotron Institute Radiation Effects Facility](#), webpage.
7. Ziegler, James F, [The Stopping and Range of Ions in Matter \(SRIM\) software simulation tool](#), webpage.
8. D. Kececioglu, "Reliability and Life Testing Handbook", Vol. 1, PTR Prentice Hall, New Jersey, 1993, pp. 186-193.
9. Vanderbilt University, [ISDE CRÈME-MC](#), webpage.
10. A. J. Tylka, J. H. Adams, P. R. Boberg, et al., "CREME96: A Revision of the Cosmic Ray Effects on Micro-Electronics Code", *IEEE Trans. on Nucl. Sci.*, Vol. 44(6), Dec. 1997, pp. 2150-2160.
11. A. J. Tylka, W. F. Dietrich, and P. R. Boberg, "Probability distributions of high-energy solar-heavy-ion fluxes from IMP-8: 1973-1996", *IEEE Trans. on Nucl. Sci.*, Vol. 44(6), Dec. 1997, pp. 2140-2149.

## IMPORTANT NOTICE AND DISCLAIMER

TI PROVIDES TECHNICAL AND RELIABILITY DATA (INCLUDING DATA SHEETS), DESIGN RESOURCES (INCLUDING REFERENCE DESIGNS), APPLICATION OR OTHER DESIGN ADVICE, WEB TOOLS, SAFETY INFORMATION, AND OTHER RESOURCES "AS IS" AND WITH ALL FAULTS, AND DISCLAIMS ALL WARRANTIES, EXPRESS AND IMPLIED, INCLUDING WITHOUT LIMITATION ANY IMPLIED WARRANTIES OF MERCHANTABILITY, FITNESS FOR A PARTICULAR PURPOSE OR NON-INFRINGEMENT OF THIRD PARTY INTELLECTUAL PROPERTY RIGHTS.

These resources are intended for skilled developers designing with TI products. You are solely responsible for (1) selecting the appropriate TI products for your application, (2) designing, validating and testing your application, and (3) ensuring your application meets applicable standards, and any other safety, security, regulatory or other requirements.

These resources are subject to change without notice. TI grants you permission to use these resources only for development of an application that uses the TI products described in the resource. Other reproduction and display of these resources is prohibited. No license is granted to any other TI intellectual property right or to any third party intellectual property right. TI disclaims responsibility for, and you will fully indemnify TI and its representatives against, any claims, damages, costs, losses, and liabilities arising out of your use of these resources.

TI's products are provided subject to [TI's Terms of Sale](#) or other applicable terms available either on [ti.com](https://www.ti.com) or provided in conjunction with such TI products. TI's provision of these resources does not expand or otherwise alter TI's applicable warranties or warranty disclaimers for TI products.

TI objects to and rejects any additional or different terms you may have proposed.

Mailing Address: Texas Instruments, Post Office Box 655303, Dallas, Texas 75265  
Copyright © 2024, Texas Instruments Incorporated